

NJC

Accepted Manuscript



This is an *Accepted Manuscript*, which has been through the Royal Society of Chemistry peer review process and has been accepted for publication.

Accepted Manuscripts are published online shortly after acceptance, before technical editing, formatting and proof reading. Using this free service, authors can make their results available to the community, in citable form, before we publish the edited article. We will replace this *Accepted Manuscript* with the edited and formatted *Advance Article* as soon as it is available.

You can find more information about *Accepted Manuscripts* in the [Information for Authors](#).

Please note that technical editing may introduce minor changes to the text and/or graphics, which may alter content. The journal's standard [Terms & Conditions](#) and the [Ethical guidelines](#) still apply. In no event shall the Royal Society of Chemistry be held responsible for any errors or omissions in this *Accepted Manuscript* or any consequences arising from the use of any information it contains.



www.rsc.org/njc

ARTICLE

Electrochemical sensor rhodamine B hydrazide-immobilized graphene oxide for highly sensitive and selective detection of Cu (II)

Cite this: DOI: 10.1039/x0xx00000x

Received 00th January 2012,
Accepted 00th January 2012

DOI: 10.1039/x0xx00000x

www.rsc.org/

Mengmeng Kang^a, Donglai Peng^{a, b}, Yuanchang Zhang^a, Yanqin Yang^b, Linghao He^a, Fufeng Yan^a, Shumin Sun^a, Shaoming Fang^{a, b}, Peiyuan Wang^{a, b*}, Zhihong Zhang^{a, b*}

A novel strategy for fabricating a Cu²⁺ sensor based on rhodamine B hydrazide (RBH)-immobilized graphene oxide (GO) was reported. The thiol-modified Au electrode was functionalized by carboxyl functionalized GO through intermolecular interaction, followed by the chemical bonding with RBH. The developed nanocomposite was used as an electrochemical sensor for detecting Cu²⁺ in aqueous solution using electrochemical impedance spectroscopy analysis with a detection limit of 0.061 nM within a range from 0.1 to 50 nM. Furthermore, the interference from potentially interfering ions such as Hg²⁺, Ag⁺, Cr²⁺, Fe²⁺, Pb²⁺, Ba²⁺, Mn²⁺, Co²⁺, and Ni²⁺ associated with Cu²⁺ analysis could be effectively inhibited. In addition, the developed Cu²⁺ sensor could be reproduced up to 10 cycles. For this approach, the fluorescent probe RBH can be replaced by another fluorescein derivatives which could identify corresponding ions, which makes the approach a widely applicable strategy for metal ion detection.

1. Introduction

In recent years, significant efforts have been dedicated to the detection of Cu²⁺ ions in environmental and biological systems owing to their possible toxic effect on human health. It has been evidenced that high level of Cu²⁺ can lead to the disturbance of cellular homeostasis. Thus far, various efficient and reproducible methods, such as atomic absorption spectrometry¹, inductively coupled plasma mass spectrometry (ICPMS)², and inductively coupled plasma atomic emission spectrometry (ICP-AES)³⁻⁵, have been developed for the detection of heavy metal ions. However, those methods require expensive and sophisticated instruments that limit their extensive use. Moreover, considerable attention has been devoted to the design of efficient and selective colorimetric chemosensors for Cu²⁺ due to its simplicity as well as the quick and nondestructive advantages of the adsorption method.

As a result, increasing attention has recently been focused on the design of high sensitive sensors for heavy metal ions, including those based on organic fluorophores, quantum dots, peptides, and DNA. Among these, rhodamines comprise an important class of fluorogenic and chromogenic probes, which are the ideal platforms for the development of colorimetric chemosensors for specific heavy and transition metal ions. Utilization of rhodamine spirolactam ring-opening process for the detection of metal ions has been well documented⁶⁻⁹.

Particularly, sensors based on the chemical species induced changes in fluorescence appear to be particularly attractive due to the highly sensitive, quick, simple and real time monitoring of the fluorescence. A large number of rhodamine-based "turn-on" chemosensors and chemodosimeters for transition- or heavy-metal ions have been developed in recent years^{9, 10}. As the excellent structural and photophysical properties of rhodamine derivatives, the search for new rhodamine sensors with the characteristics of high selectivity and affinity, sensitive and reversible turn-on response to analytic species, as well as good water-solubility, and broad pH range has been the focus of extensive investigation¹¹. Rhodamine-based derivative bearing a pyrene group as a chemosensor for Cu²⁺, in which the rhodamine ring-opening process was introduced to give a colorimetric change and "turn-on" fluorescence signal toward Cu²⁺ was reported^{9, 12}.

¹Henan Provincial Key Laboratory of Surface and Interface Science.

²Henan Collaborative Innovation Center of Environmental Pollution Control and Ecological Resoration.

Zhengzhou University of Light Industry, No. 166, Science Avenue, Zhengzhou 450001, P. R. China

Corresponding author

Tel.: +86-37186609676 Fax: +86-37186609676

*E-mail addresses: mainzhzh@163.com or

peiyuanwang@zzuli.edu.cn

Compared with routine methods, electrochemical impedance spectroscopy (EIS) is a powerful method of analyzing the complex electrical resistance of a system and is sensitive to surface phenomena and changes of bulk properties¹³. It has been intensively used, for example, for the elucidation of corrosion mechanisms¹⁴, the characterization of charge transport across membranes and membrane/solution interfaces¹⁵, and biomolecular detection of biosensors¹⁶. In the field of sensors, it is particularly well-suited to the detection of binding events on the transducer surface, and it has shown high sensitivity^{17, 18}. However, the poor electrochemical performance of the rhodamine will reduce the sensitive of the electrochemical sensors. Based on this, we introduce nanomaterials with good electrochemical performances to construct electrochemical sensors.

To the best of our knowledge, no report about rhodamine as electrochemical sensor for the metal ions detection has been published. Furthermore, graphene oxide (GO) has been studied in the context of many applications, such as field-effect transistors, composites, biosensors, due to its excellent electrical, mechanical, and thermal properties^{19, 20}. Chemically, GO has plenty of oxygen atoms on the graphitic backbone in the forms of epoxy, hydroxyl, and carboxyl groups²¹. These oxygen groups can bind to metal ions, especially the multivalent metal ions for example, Ca^{2+} , Mg^{2+} , Co^{2+} , Cd^{2+} , through both electrostatic and coordinate approaches²²⁻²⁶. However, GO also has bad selectivity to metal ions²³. Therefore, we designed a new kind of electrochemical sensor based on the complex of GO and rhodamine B hydrazide (RBH), which was used to detect Cu^{2+} in the aqueous solution. Here GO was selected to improve the electrochemical performance and adsorb Cu^{2+} . GO contains a range of reactive oxygen functional groups, which renders it a good candidate for use in the aforementioned applications (among others)

through chemical functionalization. Additionally, the alkane molecules with short alkyl chains, such as tridecane ($\text{C}_{13}\text{H}_{28}$), tetradecane ($\text{C}_{14}\text{H}_{30}$), and pentadecane ($\text{C}_{15}\text{H}_{32}$), can form lamellar structures on graphene²⁷. It demonstrates that GO could be attached to the electrode surface by this kind of the intermolecular interaction. We present a technique for the highly selective and sensitive detection of Cu^{2+} using rhodamine. The developed electrochemical sensor was used to detect Cu^{2+} and showed high sensitivity and selectivity toward other inference metal ions.

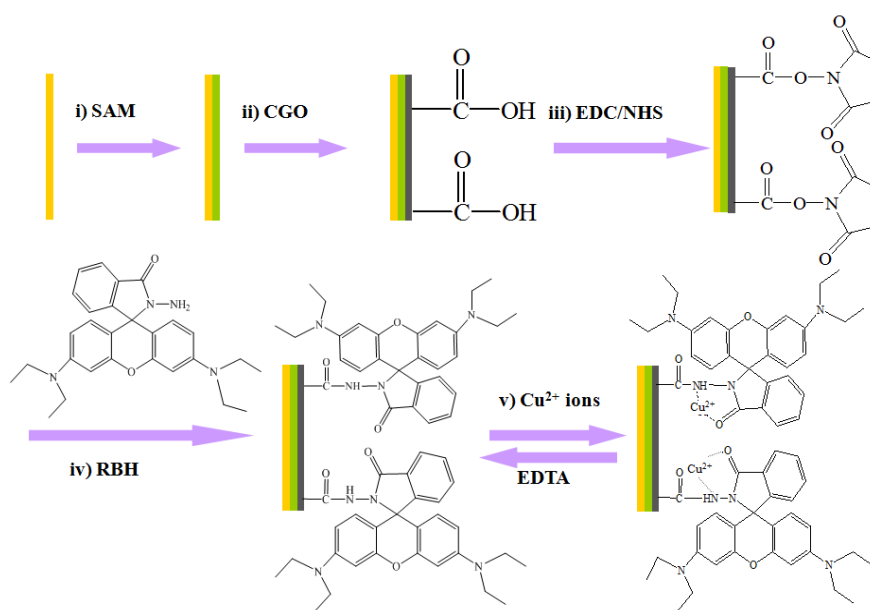
2. Materials and Methods

2.1 Reagents

1-octadecanethiol (ODT), mercaptohexadecanoic acid (MHA), $\text{K}_3[\text{Fe}(\text{CN})_6]$, and $\text{K}_4[\text{Fe}(\text{CN})_6]\cdot\text{H}_2\text{O}$ were purchased from Alfa Aesar (Shanghai, China). Graphite micro-powder, N-hydroxysulfosuccinimide (NHS), 1-ethyl-3-(3-dimethylaminopropyl) carbodiimide hydrochloride (EDC), and Ethylene Diamine Tetraacetic Acid (EDTA) were purchased from Sinopharm Chemical Reagent Co., Ltd. (Shanghai, China). RBH and the other reagents, which were of analytical-reagent grade, were purchased from Sigma-Aldrich (Shanghai, China) and used without further purification. Water was obtained from a Millipore water purification system ($\geq 18.2 \text{ M}\Omega$, Milli-Q, Millipore) and used in all runs.

2.2 Preparation of phosphate buffer, and electrolyte solutions

Phosphate buffer solution (PBS; pH 7.4) was prepared by mixing 1/15 M Na_2HPO_4 and 1/15 M KH_2PO_4 in $v(\text{Na}_2\text{HPO}_4):v(\text{KH}_2\text{PO}_4) = 8:2$. The electrolyte solution was immediately prepared before use by dissolving 1.65 g of $\text{K}_3[\text{Fe}(\text{CN})_6]$ and 2.11 g of $\text{K}_4[\text{Fe}(\text{CN})_6]$ in 1 L of PBS.



Scheme 1 Schematic of the modified electrode and its putative interaction with metal ions.

2.3 Preparation of carboxyl functionalized GO (CGO)

GO was prepared from a modified Hummers method and description in the Supporting Information²⁸. CGO was prepared according to the previous report²⁹. In brief, 0.1 g GO was dispersed in 100 mL alcohol solution and ultrasonic 1h. 50 mg ClCH₂COONa was dissolved in 1 mL GO suspension (1 mg·mL⁻¹), followed by ultrasonic for 2 h. Subsequently, the mixed solution was adjusted to neutral by adding hydrochloric acid. The solution was centrifuged 5 times until the product is well-distributed in milli-Q water. Finally, the suspension was dialyzed with milli-Q water to remove impurity ions for 48 h, and dried in an oven at 60 °C for 24 h. The powder of CGO was grinded before use.

2.4 Stepwise preparation of RBH-CGO-modified Au electrode

The pretreatment of the Au electrode was undertaken by following published procedures³⁰. The Au electrode was polished successively with 0.5 and 0.03 μm alumina slurries made from alumina powder and water on micro cloth pads. After removal of the alumina from the surface with copious amounts of water, it was briefly cleaned in an ultrasonic bath with ethanol and water between polishing steps. Subsequently, the Au electrode was cleaned in 0.5 M H₂SO₄ by cycling the electrodes between -0.3 and 1.5 V until a reproducible voltammogram was obtained. The Au electrode was washed off with milli-Q water and dried under a stream of nitrogen.

The modification of Au electrode by CGO and RBH includes four steps (**Scheme 1**). i) When the pre-treated Au electrode was immersed in ethanol solution containing 0.01 M ODT for 0.5 h, the self-assembled monolayer (SAM) of ODT on the surface of Au electrode (Au-ODT) via the formation of the Au-S covalent bond between the thiol group of ODT and Au atom was formed; ii) Au-ODT was immersed in ethanol solution containing 1 g·L⁻¹ CGO for 1 h to ensure that could be bonded with the alkyl chains of ODT by the intermolecular interaction, leading to a large number of -COOH remained on the surface of the Au electrodes modified with CGO (Au-ODT-CGO); iii) Au-ODT-CGO was put into 100 μL PBS solution containing 0.4 M EDC and 0.1 M NHS and incubated for 1 h at room temperature in order to activate the -COOH of CGO through the formation of an NHS ester intermediate (Au-ODT-ACGO)^{21, 31}; and iv) Au-ODT-ACGO was immersed in a ethanol solution containing 10 μM RBH to produce the RBH-modified electrode (Au-ODT-ACGO-RBH).

2.5 Characterization studies

X-ray photoelectron spectroscopy (XPS) was used to confirm the variation of the chemical structure of the modified Au electrode. The XPS-analysis was conducted using a VG Scientific ESCA 2000 spectrometer with an Mg-K^α X-ray source set at 170 W (13 mA and 13 kV). All spectra were referenced to the main C 1s peak, which was assigned a value of 284.6 eV.

2.6 Electrochemical measurements

All electrochemical measurements were performed with a conventional three-electrode cell with a CHI 660D electrochemical workstation (CHI Instruments, Shanghai, China). The modified Au electrode served as the working electrode. A platinum foil and an Ag/AgCl (saturated KCl solution) electrode were used as auxiliary electrode and reference electrode, respectively. Electrochemical impedance spectroscopy (EIS) data were obtained in the frequency range from 0.01 Hz to 100 kHz with alternating current amplitude of

5 mV. The measurement was applied at the formal potential of Fe(CN)₆^{4-/3-} in 5 mM Fe(CN)₆⁴⁺ + Fe(CN)₆³⁻ (1:1) solution in PBS (pH 7.4, containing 0.1 M KCl). The spectra were analyzed using Zview2 software, which uses a nonlinear least-squares fit to determine the parameters of the elements in the equivalent circuit.

2.7 Metal ions sensing

Copper dichloride (CuCl₂) was used to supply Cu²⁺ ions for detection. 1.7g CuCl₂ was resolved in 10 mL milli-Q water, a stock solution of CuCl₂ (1 mM) was prepared. Various concentrations (0.1, 0.5, 1, 5, 10, and 50 nM) were obtained by serial dilution of the stock solution. The limitation detection measurement was done by EIS when the modified Au electrode was immersed in K₃[Fe(CN)₆]/K₄[Fe(CN)₆] buffer solution with different concentrations of Cu²⁺ ions for at least 50 min, and washed with PBS solution (**Scheme 1 v**). Following metal ions were added as chlorides to evaluate the specificity of the probe: Hg²⁺, Ag⁺, Cr²⁺, Fe²⁺, Pb²⁺, Ba²⁺, Mn²⁺, Co²⁺, and Ni²⁺ with the concentration of 10 μM. After the detection of Cu²⁺ ions, the modified electrode was placed in 0.1 M EDTA solution for regeneration (**Scheme 1 v**), then rinsed carefully. It was measured by EIS in a blank solution of PBS to ensure complete stripping of all ions.

3 Results and discussion

3.1 Chemical structure of samples at different stages

XPS technique was used to characterize the variation of the surface chemical property³² during the procedure of the sensing layer fabrication for Cu²⁺ ions detection. The fitted C 1s and N 1s core-level XPS spectra of samples at different stages, namely, (a) CGO, (b) activated CGO (ACGO), (c) RBH functionalized CGO (GO-RBH), and (d) GO-RBH-Cu²⁺ are summarized in Fig. 1. For CGO and ACGO samples, the same fitted peak is mainly at ~284.6 eV, which assigns to C-C/C-H/C-S bonds. Three additional peaks were observed in C 1s of ACGO [Fig. 1 (b)] at higher binding energy, ~286, ~287.7, and ~288.8 eV, which are attributed to C-O (ether), C=O (carbonyl), and O-C=O (ester). Among the three peaks, ether and carbonyl groups may be from GO, whereas ester groups could have resulted from the transformation of carboxyl groups in GO activated by EDC/NHS. In the case of the sample of GO-RBH and GO-RBH-Cu²⁺, the peak at ~288.8 eV (ester group) disappeared, whereas a substantial N 1s signal was observed, as shown in Fig.1 (c) and (d). When RBH reacted with the activated surface containing esters, N-C=O groups (amide) could be produced between them, which maybe has been included in the peak at ~287.7 eV together with the carbonyl group. The small peaks at 285.2 eV correspond to C=N bonds.³³ Additionally, C-N groups could be contained in the peak at ~286.2 eV with C-O bonds. Both -N-C=O (amine) and C-N (primary, secondary, or tertiary amine groups) groups were obtained by fitting the N 1s core-level XPS spectrum, which are at ~399.96 and 401.66 eV, respectively. Another peak at ~399.5 eV in the N 1s spectrum was fitted out and could be contributed to C=N (imine) group, which could be the final product of the reaction of the amino groups in RBH and the ester groups on the sensor surface³⁴. The peak area ratio of peaks at ~399.5 and ~399.96 eV in the fitted N 1s spectrum [Fig. 1 (c')] is

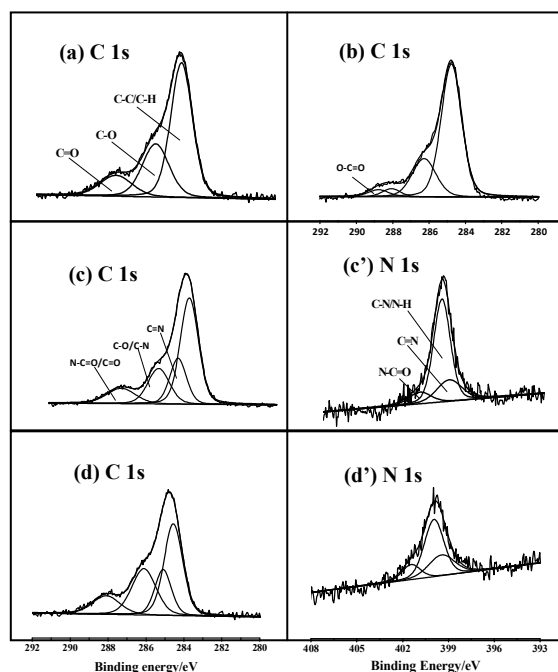


Fig. 1 C 1s and N 1s core-level XPS spectra of samples at different steps: (a) CGO, (b) ACGO, (c) GO-RBH, and (d) GO-RBH-Cu²⁺ sensor, respectively.

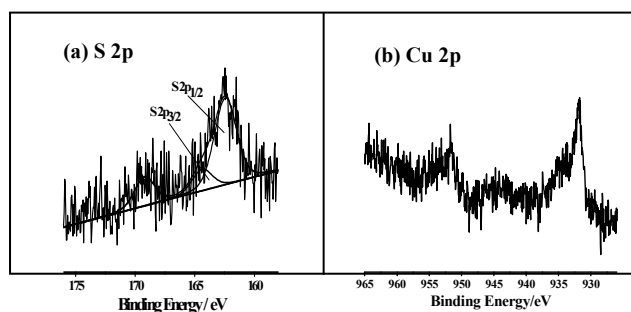


Fig. 2 (a) S 2p core-level XPS spectrum of all samples and (b) Cu 2p core-level XPS spectra of the GO-RBH-Cu²⁺ sample.

Table 1 Atomic % of samples at different stages: a) CGO, b) ACGO, c) GO-RBH, and d) GO-RBH-Cu²⁺

Sample	Atomic %			
	C 1s	O 1s	N 1s	Cu 2p
CGO	97.52	7.21	-	-
ACGO	70.73	24.87	-	-
GO-RBH	61.09	28.44	7.69	-
GO-RBH-Cu ²⁺	58.77	27.22	7.82	0.96

approximately 2.1. This suggests that approximately 2/3 amide groups in GO-RBH films were transferred to imine groups³⁵. Before RBH was bonded with ACGO, however, no peak in N1s core-level XPS spectrum is corresponding to N-C group (Fig. S1).

Additionally, a signal of S 2p core-level XPS spectrum in all samples was observed (Fig. 2a), which is deduced from the thiol-

groups in ODT self-assembled onto the Au electrode surface. When the RBH-functionalized GO-RBH was used to detect Cu²⁺ ions, a clear signal of Cu 2p is determined by XPS (Fig. 2b), which has two peaks at ~931.9 and ~934.1 eV belong to the active Cu³⁶. These results confirm that RBH could be bonded onto the functionalized surface and could be used as the sensing layer for Cu²⁺ detection.

The atomic % of all samples at different stages is summarized in Table 1, which could reveal the variation of the elements in samples during the fabrication of the sensing surface based on GO-RBH. The table shows that C % decreases from the range of 97.52% to 58.77% while the procedure was going on. The result could be explained by the participation of O and N together with the complex chemical structure. The oxygen content increased substantially from 7.21% to 24.87% after CGO bonded with the alkyl-functionalized surface. The increase was mainly due to the presence of oxygen-related groups in CGO, which could also be proved by C 1s XPS spectrum of CGO, as previously discussed. Afterward, O and N contents were kept constant in the samples of GO-RBH and GO-RBH-Cu²⁺. Moreover, 0.96% Cu was detected by XPS when the GO-RBH layer was used to detect Cu²⁺.

3.2 Electrochemical performances of Cu²⁺ sensor at different stages

EIS measurements of the samples at the different stages were carried out to investigate the capability of electron transfer changes of different electrodes during the procedure of the sensing fabrication (Fig. 3). The EIS spectra of the electrodes are composed of a semicircle and a straight line featuring a diffusion-limiting step of the Fe(CN)₆^{4-/3-} process. The spectra were simulated using the Randles equivalent circuit consisting of solution resistance (R_s), charge-transfer resistance (R_{ct}), constant-phase element (CPE), and the Warburg impedance (W), as shown in the inset of Fig. 3. Moreover, the calculated values for these elements are shown as Table S1 in Supporting Information. The result shows that the R_{ct} of the bare Au electrode is only 94.2 ohm, an almost straight line which is characteristic of a diffusion limited electrochemical process³⁷. After the formation of Au-ODT, however, the R_{ct} value increases to 4.11 kohm. This could be explained by the coverage effect of the insulated organic molecules on the electrode surface, which further resists the electron transfer at the interface.³⁸ Meanwhile, the addition of ODT would increase the film thickness, leading to a higher R_{ct} value³⁹. When CGO bonded with alkyl groups of ODT by the intermolecular interaction onto the surface of Au electrode, the R_{ct} value is 1.95 kohm. The relative low R_{ct} of Au-ODT-CGO indicates the rapid electron transfer at the interface between the the modified electrode and the electrolyte solution. It is mainly attributed to excellent conductivity and good compatibility of graphene-related nanomaterials.⁴⁰ When -COOH of CGO were activated through the formation of an NHS ester intermediate³¹, EDC-NHS has a more complex crosslinking mechanism and acts like a catalyst: EDC first covalently attaches to the -COOH groups present on the surface of the modified electrode, which then reacts with NHS, substituting EDC, covalently attaching to the functionalised electrode surface whilst releasing 1-(3-dimethylamino)propyl-3-ethylurea. EDC-NHS crosslinked CGO films the electron transfer is facilitated.⁴¹ Consequently, the R_{ct} value obviously decreased to 0.25 kohm⁴². Successively,

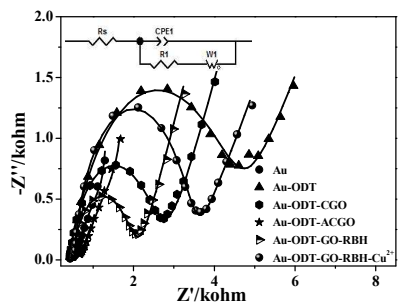


Fig. 3 (a) Nyquist plot of EIS in $K_3[Fe(CN)_6]/K_4$ (1:1) mixture and PBS (pH 7.4, containing KCl) in the frequency range from 0.01 Hz to 100 kHz with 5 mV amplitude: bare Au electrode, Au-ODT, Au-ODT-CGO, Au-ODT-ACGO, Au-ODT-GO-RBH, and Au-ODT-GO-RBH- Cu^{2+} . The inset is the equivalent circuit of the Nyquist plot, and the calculated values for these elements are shown in the Table S1 of the Supporting Information.

such structures facilitate RBH reaction in which it substitutes NHS, in this way covalently “gluing” the electrode surface with RBH amino groups, releasing unchanged NHS. The R_{ct} value increased to 1.42 kohm, which is mainly due to the insulation of the RBH molecules of the modified and thick layer^{39, 43}. After the addition of Cu^{2+} in the system of Au-ODT-CGO-RBH, it gave a slightly higher R_{ct} with a value of 2.62 kohm.

The adsorption mechanism of Cu^{2+} on RBH was shown as Fig. S4. Upon addition of Cu^{2+} to a solution of hydrazide **1** in acetonitrile, Cu(II) induces a $1 \rightleftharpoons 3$ equilibrium in much the same way that the proton induces an analogous rhodamine B equilibrium in water. The reaction with Cu(II) in water (as compared to acetonitrile as described above) predictably **2** effects a redox hydrolysis of **3** leading to rhodamine B (**4**) itself in a stoichiometric **3** process.⁴⁴ As a result, negative charges were observed on **3** and **4**. Negative charged electron at the Au-ODT-ACGO-RBH interface would electro-statically repel negatively charged redox species in solution. This repulsion modulates the access of the redox species to the interface, hence leading to a decrease in the electrontransfer rate reflected by an enhanced charge transfer resistance, R_{ct} , in the EIS.⁴⁵ The data of Nyquist plots for EIS in the procedure of the Cu^{2+} detection were summarized in Fig. S2.

Additionally, RBH was also functionalized directly on MHA which was self-assembled onto the Au electrode without GO layer (Fig S2 (a)). In order to compare the above results, the adsorption of Cu^{2+} onto the pristine GO was carried out (Fig S2 (b)). It demonstrates that the R_{ct} values of the Au electrode modified by MHA-RBH were substantially higher than those of GO-RBH system, which could be due to the poor transfer activity of the electrons at the interface of the electrolytes solution and the modified electrode⁴⁶. Successively, it will restrict the application of this kind of electrochemical sensor in the detection of heavy metals. For the sensor based on the pristine GO layer, only a slight change of R_{ct} value before and after Cu^{2+} detection was observed. It was found the change of R_{ct} produced by Cu^{2+} adsorption on GO-RBH was higher than that of GO, indicating that the presence of GO could improve the electrochemical activity

performance of the sensor. Furthermore, carboxyl functionalized carbon nanotube modified with RBH was used to detect Cu^{2+} , which was determined by EIS and shown in Fig S3. It demonstrates that the difference of R_{ct} before and after the addition of Cu^{2+} of 1.81 kohm was observed and smaller than that of the composite electrode modified with GO-RBH (Table S3). It also indicates the Cu^{2+} detection using GO-RBH exhibits relatively high efficiency.

3.3 Detection dynamics of Cu^{2+} using the developed sensor

It is advantageous to use EIS for ionic recognition in the case of the RBH-modified electrodes because this method is water compatible and allows for facile detection of target ion⁴⁷. Our preliminary EIS spectra showed that RBH sensor has a good selectivity to Cu^{2+} in milli-Q water. As shown in Fig. 4(a) are the EIS spectra of the modified electrodes during incubation with 10 mL PBS solution containing 10 μM Cu^{2+} . After immersing the RBH-modified Au electrode in a solution containing Cu^{2+} , the R_{ct} value increased remarkably to 3.84 kohm. With the incubation time going on, the diameter of the semi-circles in EIS decreased, indicating the increase the transfer activity of the electrons at the interface between the electrolytes solution and the modified electrode with GO-RBH. Actually, Cu^{2+} may be absorbed onto the layer of graphene layer not only coordinated with RBH²⁶. In consequence, more and more Cu^{2+} would approach to GO layer with the time going on due to the effect of the precipitation on the carbon layer leading to the decrease of the R_{ct} value, as mentioned above⁴⁸. The R_{ct} value in the equivalent circuit was obtained through Zview2 software and summarized in Fig. 4(b). The R_{ct} value reaches to equilibrium after approximately 80 min. Thus, an incubation time of 80 min was used for all subsequent experiments. It should be noted that a longer incubation time was obtained in comparison with that of UV-vis adsorption spectroscopy⁴⁹.

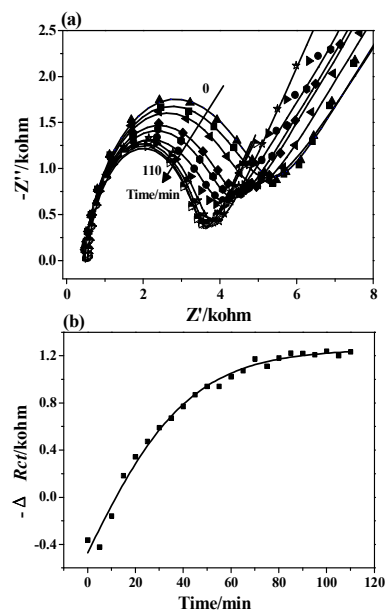


Fig. 4 (a) Nyquist plot of EIS in 5 mM $K_3[Fe(CN)_6]/K_4[Fe(CN)_6]$ (1:1) mixture and PBS (pH 7.4, containing 0.1 M KCl) in the frequency range from 0.01 Hz to 100 kHz with 5 mV amplitude of the GO-RBH modified electrode

for the detection of Cu^{2+} ions ($10 \mu\text{M}$) during incubation. (b) Effect of the incubation time on the simulated R_{ct} values.

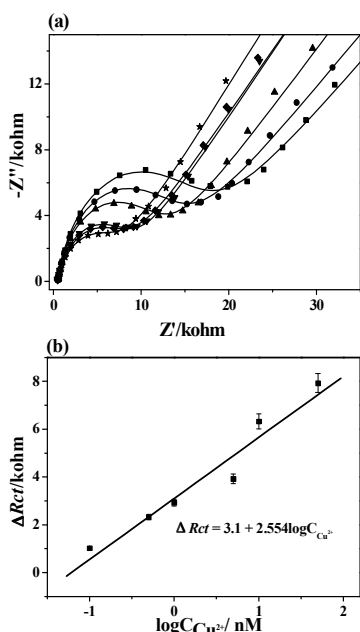


Fig. 5 (a) Nyquist plot for EIS in 5 mM $\text{K}_3[\text{Fe}(\text{CN})_6]/\text{K}_4[\text{Fe}(\text{CN})_6]$ (1:1) mixture and PBS (pH 7.4, containing 0.1 M KCl) in the frequency range from 0.01 Hz to 100 kHz with 5 mV amplitude of the GO-RBH modified electrode for the detection of Cu^{2+} ions at different concentrations of 0.1, 0.5, 1, 5, 10, and 50 nM. (b) Linear calibration curve for ΔR_{ct} versus $\lg C_{\text{Cu}^{2+}}$, where $C_{\text{Cu}^{2+}}$ is the concentration of Cu^{2+} ions.

3.4 Sensitivity of the Cu^{2+} sensor determined by EIS

The quantitative behavior of this new assay was assessed by determining the dependence of the ΔR_{ct} of the modified Au electrode before and after Cu^{2+} detection on the amount of Cu^{2+} ions. After RBH reacted with the ACGO surface, Cu^{2+} with different concentrations was subsequently incubated into the system, followed by measurements by EIS (Fig. 5). The electron-transfer resistance increased with the increase of Cu^{2+} concentrations as shown in Fig. 5. It may be due to more Cu^{2+} binding to the immobilized RBH in higher Cu^{2+} concentrations, which acts as a definite kinetic barrier for the electron transfer.⁵⁰ The phenomenon was consistent with the previously described. The sensitivity of the developed Cu^{2+} sensor was deduced on the basis of the values obtained for detection and quantification limits. The limit of detection (LOD) could be calculated based on the parameters obtained from the regression curve. The linear curve fitted a regression equation of $\Delta R_{ct} = 3.1 + 2.554 \lg C_{\text{Cu}^{2+}}$ within a range from 0.1 nM to 50 nM with a correlation coefficient of $R^2 = 0.95359$, where $C_{\text{Cu}^{2+}}$ is the concentration of Cu^{2+} ions. LOD was 0.061 nM at a signal-to-noise ratio of 6, which is comparable with those of most previous assay techniques (Table 2). The sensitivity also is significantly lower than the maximum level ($\sim 20 \mu\text{M}$) of Cu^{2+} in drinking water permitted by the U.S. Environmental Protection Agency (EPA)⁵¹.

3.5 Selectivity of the Cu^{2+} sensor

Table 2 Previous assay techniques for the detection of Cu^{2+}

Sensitive layer	Detection Technology	Linear range	LOD	References
Rhodamine pirolactam derivative	Colorimetric	0.8-10 μM	0.3 μM	52
Rhodamine-based Cu^{2+} sensors	fluorescence spectroscopy	50 nM-8 μM	30 nM	53
Rhodamine dye	UV-visible absorbance spectra	0 nM-0.01 M	1.1 nM	54
Graphitic Carbon Nitride Nanorods	photoelectrochemical	0.018-55 μM	6.2 nM	55
Molecularly imprinted polymer	QCM	1 nM-50 μM	80 nM	56
DNAzyme	EIS	6.5-40 μM	0.04 μM	57

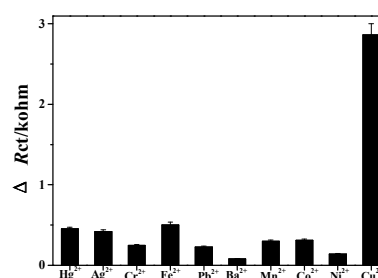


Fig. 6 Selectivity of the Cu^{2+} sensing system. The concentration of Cu^{2+} or other metal ions is $10 \mu\text{M}$.

The selectivity of the sensor was studied by the system against other possible interfering ions in the real sample, e.g., Hg^{2+} , Ag^+ , Cr^{2+} , Fe^{2+} , Pb^{2+} , Ba^{2+} , Mn^{2+} , Co^{2+} , and Ni^{2+} . In this case, the comparison was performed by assaying $10 \mu\text{M}$ interfering materials with target Cu^{2+} ions by EIS. High signal of ΔR_{ct} in the detection of metal ions could be obtained toward target Cu^{2+} (Fig 6). The potentially interfering ions in water system showed no apparent interference in the detection of Cu^{2+} . Therefore, the selectivity of the sensor was acceptable.

3.6 Repeatability

After each measurement, the regeneration of metal-free electrodes was achieved by soaking the used electrode in EDTA solution. Almost all Cu^{2+} ions were removed from the electrode by EDTA-mediated regeneration process (Fig. 7). The procedure was repeated 10 times continuously. The result suggests that the response signal to the same concentration of Cu^{2+} ions could be recovered. Each electrode could be used in the determination of metal ions over a couple of days without significant loss of sensitivity. It is also comparable with the electrochemical biosensor based on the DNAzyme for detecting heavy metal ions.⁵⁸⁻⁶⁰

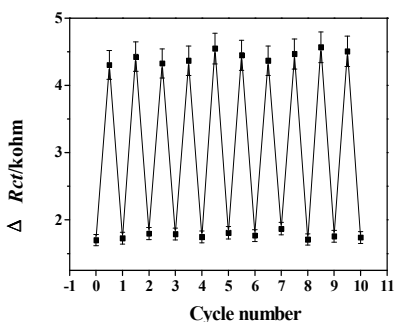


Fig. 7 Reusability of the RBH-based Cu^{2+} sensor challenged with $10 \mu\text{M}$ Cu^{2+} and washed with 0.1 M EDTA.

4. Conclusions

We reported a novel graphene oxide-modified Au modified with rhodamine B hydrazide using successive self-assembled monolayer of alkyl chains, graphene oxide containing carboxyl groups by the intermolecular interaction, and chemical bonding of RBH. The prepared electrode exhibited high detection sensitivity with the lowest detection limit of 0.061 nM for Cu^{2+} ions within the range from 0.1 to 50 nM . The developed new electrode showed good stability and reusability. Excellent selectivity toward interfering metal ions such as Hg^{2+} , Ag^+ , Cr^{2+} , Fe^{2+} , Pb^{2+} , Ba^{2+} , Mn^{2+} , Co^{2+} , and Ni^{2+} can be achieved. For this approach, the fluorescent probe can be replaced by another, making this approach a widely applicable strategy for metal ion detection.

Acknowledgements

This work was supported by Program for the National Natural Science Foundation of China (NSFC: Account No. 51173172 and 21104070) and Science and Technology Opening Cooperation Project of Henan Province (Account No. 132106000076).

Notes and references

^a Henan Provincial Key Laboratory of Surface and Interface Science

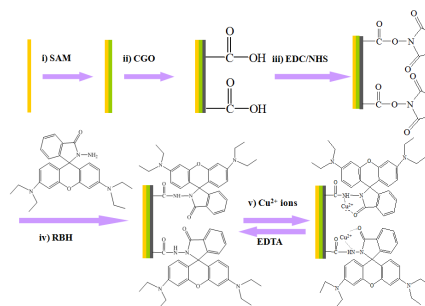
^b Henan Collaborative Innovation Center of Environmental Pollution Control and Ecological Restoration
Zhengzhou University of Light Industry, No. 166, Science Avenue, Zhengzhou 450001, P. R. China

- A. T. Duarte, M. B. Dessuy, M. G. R. Vale, B. Welz and J. B. de Andrade, *Talanta*, 2013, **115**, 55-60.
- J. Mattusch and R. Wennrich, *Analytical Chemistry*, 1998, **70**, 3649-3655.
- B. Fairman and A. Sanz-Medel, *Fresenius J Anal Chem*, 1996, **355**, 757-762.
- R. X. Xu, X. Y. Yu, C. Gao, J.-H. Liu, R. G. Compton and X.-J. Huang, *Analyst*, 2013, **138**, 1812-1818.
- Y. Tu, Y. Zhao, M. Xu, X. Li and H. Du, *Food Anal. Methods*, 2013, **6**, 667-676.
- Y.-K. Yang, K.-J. Yook and J. Tae, *Journal of the American Chemical Society*, 2005, **127**, 16760-16761.
- J. S. Wu, I. C. Hwang, K. S. Kim and J. S. Kim, *Organic letters*, 2007, **9**, 907-910.
- X. Chen, S. W. Nam, M. J. Jou, Y. Kim, S. J. Kim, S. Park and J. Yoon, *Organic letters*, 2008, **10**, 5235-5238.
- H. N. Kim, M. H. Lee, H. J. Kim, J. S. Kim and J. Yoon, *Chemical Society Reviews*, 2008, **37**, 1465-1472.
- M. Beija, C. A. Afonso and J. M. Martinho, *Chemical Society Reviews*, 2009, **38**, 2410-2433.
- Y. Liu, Y. Sun, J. Du, X. Lv, Y. Zhao, M. Chen, P. Wang and W. Guo, *Organic & biomolecular chemistry*, 2011, **9**, 432-437.
- Y. Zhou, F. Wang, Y. Kim, S.-J. Kim and J. Yoon, *Organic letters*, 2009, **11**, 4442-4445.
- F. Lisdat and D. Schäfer, *Analytical and bioanalytical chemistry*, 2008, **391**, 1555-1567.
- R. Rettig and S. Virtanen, *Journal of biomedical materials research part A*, 2008, **85**, 167-175.
- V. Freger and S. Bason, *Journal of Membrane Science*, 2007, **302**, 1-9.
- J. A. Lee, S. Hwang, J. Kwak, S. I. Park, S. S. Lee and K.-C. Lee, *Sensors and Actuators B: Chemical*, 2008, **129**, 372-379.
- C. Tlili, H. Korri-Yousseoufi, L. Ponsonnet, C. Martelet and N. J. Jaffrezic-Renault, *Talanta*, 2005, **68**, 131-137.
- R. K. Shervedani, A. H. Mehrjardi and N. Zamiri, *Bioelectrochemistry*, 2006, **69**, 201-208.
- A. K. Geim and K. S. Novoselov, *Nature materials*, 2007, **6**, 183-191.
- S. Park and R. S. Ruoff, *Nature nanotechnology*, 2009, **4**, 217-224.
- D. R. Dreyer, S. Park, C. W. Bielawski and R. S. Ruoff, *Chemical Society Reviews*, 2010, **39**, 228-240.
- S. Park, K.-S. Lee, G. Bozoklu, W. Cai, S. T. Nguyen and R. S. Ruoff, *ACS nano*, 2008, **2**, 572-578.
- G. Zhao, J. Li, X. Ren, C. Chen and X. Wang, *Environmental science & technology*, 2011, **45**, 10454-10462.
- C. Xu, X. Wang, L. Yang and Y. Wu, *Journal of Solid State Chemistry*, 2009, **182**, 2486-2490.
- M. Machida, T. Mochimaru and H. Tatsumoto, *Carbon*, 2006, **44**, 2681-2688.
- S.-T. Yang, Y. Chang, H. Wang, G. Liu, S. Chen, Y. Wang, Y. Liu and A. Cao, *Journal of colloid and interface science*, 2010, **351**, 122-127.
- Q. Chen, H.-J. Yan, C.-J. Yan, G.-B. Pan, L.-J. Wan, G.-Y. Wen and D.-Q. Zhang, *Surface science*, 2008, **602**, 1256-1266.
- W. S. Hummers and R. E. Offeman, *J. Am. Chem. Soc.*, 1958, **80**, 1339.
- D. Du, L. Wang, Y. Shao, J. Wang, M. H. Engelhard and Y. Lin, *Analytical chemistry*, 2011, **83**, 746-752.
- S. Campuzano, R. o. Gálvez, M. a. Pedrero, F. J. M. de Villena and J. M. Pingarrón, *Journal of Electroanalytical Chemistry*, 2002, **526**, 92-100.
- A. Erdem, P. Papakonstantinou, H. Murphy, M. McMullan, H. Karadeniz and S. Sharma, *Electroanalysis*, 2010, **22**, 611-617.
- M. Seah, *Surface and Interface Analysis*, 1980, **2**, 222-239.
- K. Vasu, K. Pramoda, K. Moses, A. Govindaraj and C. Rao, *Materials Research Express*, 2014, **1**, 015001.
- D. Tu, L. Liu, Q. Ju, Y. Liu, H. Zhu, R. Li and X. Chen, *Angewandte Chemie International Edition*, 2011, **50**, 6306-6310.
- A. Chilkoti, B. D. Ratner and D. Briggs, *Chemistry of Materials*, 1991, **3**, 51-61.
- C. Weisener and A. Gerson, *Surface and interface analysis*, 2000, **30**, 454-458.
- M. Giovannini, A. Bonanni and M. Pumera, *Analyst*, 2012, **137**, 580-583.
- A. Zhu, Y. Liu, Q. Rui and Y. Tian, *Chemical Communications*, 2011, **47**, 4279-4281.
- H. Gong and X. Li, *Analyst*, 2011, **136**, 2242-2246.
- C. Karuppiyah, S. Cheemalapati, S.-M. Chen and S. Palanisamy, *Ionics*, 2015, **21**, 231-238.
- R. Pauliukaite, M. E. Ghica, O. Fatibello-Filho and C. M. Brett, *Electrochimica Acta*, 2010, **55**, 6239-6247.
- P. Geng, X. Zhang, W. Meng, Q. Wang, W. Zhang, L. Jin, Z. Feng and Z. Wu, *Electrochimica Acta*, 2008, **53**, 4663-4668.
- E. E. Ebenso, M. M. Kabanda, L. C. Murulana, A. K. Singh and S. K. Shukla, *Industrial & Engineering Chemistry Research*, 2012, **51**, 12940-12958.
- V. Dujols, F. Ford and A. W. Czarnik, *Journal of the American Chemical Society*, 1997, **119**, 7386-7387.
- M. Gebala, L. Stoica, S. Neugebauer and W. Schuhmann, *Electroanalysis*, 2009, **21**, 325-331.
- M. Chevalier, F. Robert, N. Amusant, M. Traisnel, C. Roos and M. Lebrini, *Electrochimica Acta*.
- H. JungáKim, M. HeeáLee and J. SeungáKim, *Chemical Communications*, 2010, **46**, 8448-8450.

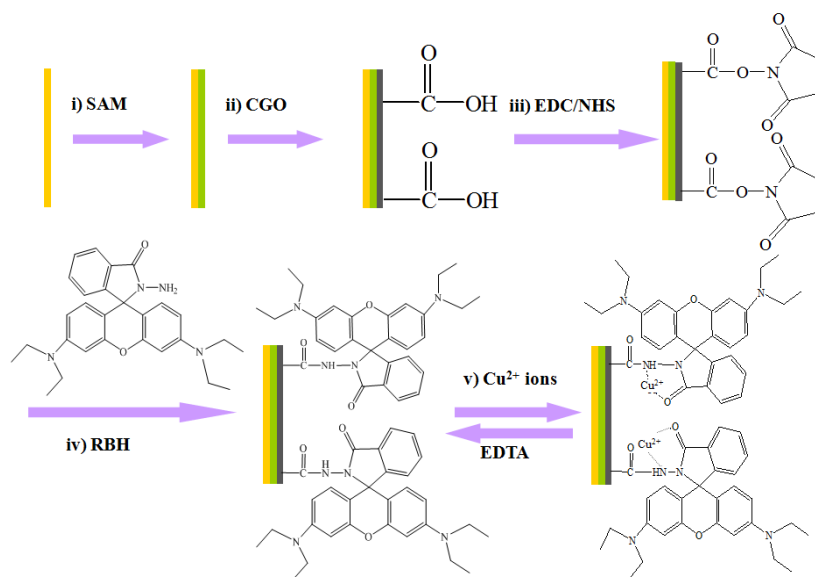
48. Y. T. Liu, M. Dang, X. M. Xie, Z. F. Wang and X. Y. Ye, *Journal of Materials Chemistry*, 2011, **21**, 18723-18729.
49. H. S. Jung, J. H. Han, Y. Habata, C. Kang and J. S. Kim, *Chemical Communications*, 2011, **47**, 5142-5144.
50. W. Jin, G. Yang, H. Shao and A. Qin, *Food Control*, 2014, **39**, 185-191.
51. C. Zong, K. Ai, G. Zhang, H. Li and L. Lu, *analytical chemistry*, 2011, **83**, 3126-3132.
52. Y. Zhao, X. B. Zhang, Z. X. Han, L. Qiao, C. Y. Li, L. X. Jian, G. L. Shen and R. Q. Yu, *Analytical Chemistry*, 2009, **81**, 7022-7030.
53. R. Narendra, S. Purna and B. Asit, *Analyst*, 2013, **138**, 1130-1136.
54. M. Min, X. Wang, Y. Chen, L. Wang, H. Huang and J. Shi, *Sensors and Actuators B: Chemical*, 2013, **188**, 360-366.
55. L. Xu, J. Xia, L. Wang, H. Ji, J. Qian, H. Xu, K. Wang and H. Li, *European Journal of Inorganic Chemistry*, 2014, n/a-n/a.
56. P. g. Su and S. d. Huang, *Spectrochimica Acta Part B: Atomic Spectroscopy*, 1998, **53**, 699-708.
57. C. Ocana, N. Malashikhina, M. del Valle and V. Pavlov, *Analyst*, 2013, **138**, 1995-1999.
58. E. Xiong, L. Wu, J. Zhou, P. Yu, X. Zhang and J. Chen, *Analytica chimica acta*, 2015, **853**, 242-248.
59. S. Fang, X. Dong, Y. Zhang, M. Kang, S. Liu, F. Yan, L. He, X. Feng, P. Wang and Z. Zhang, *New Journal of Chemistry*, 2014.
60. G. Liu, Y. Yuan, S. Wei and D. Zhang, *Electroanalysis*, 2014, **26**, 2732-2738.

ARTICLE

Table of contents entry



Electrochemical sensor rhodamine B hydrazide-immobilized graphene oxide for highly sensitive and selective detection of Cu (II).



A novel strategy for fabricating a Cu^{2+} sensor based on rhodamine B hydrazide (RBH)-immobilized graphene oxide (GO) was reported. The developed nanocomposite was used as an electrochemical sensor for Cu^{2+} detection in aqueous solution using electrochemical impedance spectroscopy analysis with a detection limit of 0.061 nM within a range from 0.1 to 50 nM.